Organometallics 1991, 10, 467-473

Synthesis and Reactivity of Ruthenium Amide–Phosphine Complexes. Facile Conversion of a Ruthenium Amide to a Ruthenium Amine via Dihydrogen Activation and Ortho Metalation. X-ray Structure of $RuCl(C_6H_4PPh_2)[NH(SiMe_2CH_2PPh_2)_2]$

Michael D. Fryzuk,[*,†] Craig D. Montgomery,[‡] and Steven J. Rettig[§]

Department of Chemistry, University of British Columbia, 2036 Main Mall, Vancouver, BC, Canada V6T 1Y6

Received June 13, 1990

The reaction of $LiN(SiMe_2CH_2PPh_2)_2$ with $RuCl_2(PPh_3)_3$ leads to the formation of the ruthenium amide complex $RuCl(PPh_3)[N(SiMe_2CH_2PPh_2)_2]$. This complex reacts with H_2 to form two isomeric amine–hydride derivatives of the formula $RuCl(PPh_3)H[NH(SiMe_2CH_2PPh_2)_2]$. Reaction of $RuCl(PPh_3)[N(SiMe_2CH_2PPh_2)_2]$ with MeLi, Me_3SiCH_2Li, or $H_2C{=}CHCH_2MgCl$ does not lead to the expected hydrocarbyl derivative; rather, ortho metalation occurs to generate $Ru(C_6H_4PPh_2)[N(SiMe_2CH_2PPh_2)_2]$. Attempts to displace the PPh_3 ligand of $RuCl(PPh_3)[N(SiMe_2CH_2PPh_2)_2]$ with PEt_3 lead to the formation of $RuCl(C_6H_4PPh_2)[NH(SiMe_2PPh_2)_2]$, having an amine ligand and the ortho-metalated phenyl group. The complex $RuCl(C_6H_4PPh_2)[NH(SiMe_2CH_2PPh_2)_2]$ crystallizes in space group $P2_1/n$ with $a = 9.8385$ (5) Å, $b = 29.561$ (1) Å, $c = 20.8665$ (9) Å, $\beta = 101.683$ (4)°, $V = 5942.2$ (5) $Å^3$, and $Z = 4$. Transformation of an amide linkage to an amide via H_2 activation or ortho metalation is apparently driven by the formation of an intramolecular hydrogen bond between the amine hydrogen and the coordinated chloride; the N—H···Cl distance is 2.76 (6) Å, which is shorter than the expected van der Waals separation of 3.0 Å.

Introduction

In the activation of dihydrogen by metal complexes, some of the most intriguing results have been obtained in ruthenium(II) chemistry. A number of d^6 halo–phosphine complexes of the type $RuCl_2(PR_3)_n$ (n = 3, 4) react with molecular hydrogen *in the presence of base* to generate hydrides with the elimination of HCl (as BH^+Cl^-).[1] Such an activation formally corresponds to the heterolytic cleavage of dihydrogen, since the metal and the base can be acting in concert to split H_2.[2] Of course, this is just a formalism, and an equally plausible mechanism could be oxidative addition of H_2 to generate a Ru(IV) dihydride complex followed by dehydrohalogenation by the base. The ambiguous nature of the mechanism by which dihydrogen is activated may apply to numerous other transition-metal complexes as well, but it is in ruthenium(II) chemistry that the ambiguity is most apparent.[3]

Employment of the mixed-donor, tridentate ligand $^-N(SiMe_2CH_2PPh_2)_2$, a basic disilylamide donor flanked by two phosphines, with rhodium and iridium has shown that reaction of dihydrogen can lead to products that are consistent with the expected results of the heterolytic cleavage of H_2.[4] For example, addition of H_2 to the iridium(III) methyl-iodide complex $Ir(CH_3)I[N(SiMe_2CH_2PPh_2)_2]$ generates an amine–hydride complex, also having the +3 formal oxidation state, as shown in eq 1. Similar results obtain for rhodium(III). However, in the case of these heavier group 9 metals, there is also the conundrum of heterolysis versus oxidative addition, as the above reaction appears to be proceeding under thermodynamic control by virtue of the *intramolecular hydrogen bond* generated between the coordinated amine N-H and the cis halide ligand. By examining the incorporation of this ligand system onto ruthenium(II), and its subsequent reactivity patterns with dihydrogen, we hoped to find other examples of the amide to amine–hydride reaction mentioned above and perhaps help distinguish the two modes of H_2 activation. In this paper, we report our findings on the preparation and reactivity of ruthenium amides.

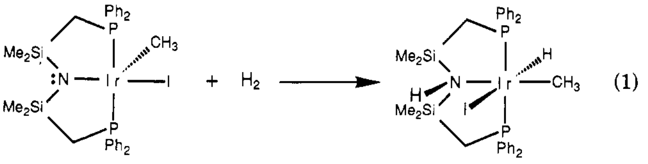

Experimental Section

General Considerations. The manipulation of all compounds was carried out under prepurified nitrogen in a Vacuum Atmospheres HE-553-2 glovebox equipped with a MO-40-2H purifier or in standard Schlenk-type glassware. $RuCl_3{\cdot}xH_2O$ was obtained from Johnson Matthey and was used to prepare $RuCl_2(PPh_3)_3$ by the standard literature method.[5] The synthesis of $LiN(SiMe_2CH_2PPh_2)_2$ was described earlier.[6]

All solvents used (hexane, toluene, and tetrahydrofuran) were dried by refluxing over sodium-benzophenone ketyl followed by distillation under Ar. In addition, THF and hexane were predried by refluxing over CaH_2. Deuterated benzene was purchased from Aldrich, dried over activated 4-Å molecular sieves, and vacuum-transferred prior to use. Allylmagnesium bromide was prepared from freshly distilled allyl bromide and excess magnesium turnings in THF, filtered through cotton wool, and standardized against 0.1 M HCl.

Elemental analyses were performed by Mr. P. Borda in this department. ^1H NMR spectra were recorded on a Bruker WH-400 (400 MHz) or a Varian XL-300 (300 MHz) spectrometer. ^{31}P

[†] E. W. R. Steacie Fellow (1990–1992).

[‡] NSERC Postdoctoral Fellow (1986–1988).

[§] Experimental Officer, UBC Crystallographic Service.

(1) Hallman, P. S.; McGarvey, B. R.; Wilkinson, G. *J. Chem. Soc. A* **1968**, 3143.

(2) Brothers, P. J. *Prog. Inorg. Chem.* **1981**, *28*, 1.

(3) James, B. R. In *Comprehensive Organometallic Chemistry*; Wilkinson, G., Ed.; Pergamon: London, 1982; Vol. 8, p 285.

(4) Fryzuk, M. D.; MacNeil, P. A.; Rettig, S. J. *J. Am. Chem. Soc.* **1987**, *109*, 2803.

(5) Hallman, P. S.; Stephenson, T. A.; Wilkinson, G. *Inorg. Synth.* **1970**, *12*, 237.

(6) Fryzuk, M. D.; MacNeil, P. A.; Rettig, S. J.; Secco, A. S.; Trotter, J. *Organometallics* **1982**, *1*, 918.

0276-7333/91/2310-0467$02.50/0

Table I. ^{1}H NMR Data

compd	SiCH_3, ppm	PCH_2, ppm	^2J(H,H), Hz	^2J(H,P), Hz	other, ppm
RuCl(PPh$_3$)[N(SiMe$_2$CH$_2$PPh$_2$)$_2$] (1)	0.06 (s)	1.74 (dt)	13.0	5.6	
	0.35 (s)	2.92 (dt)		5.7	
RuH(Cl)PPh$_3$[NH(SiMe$_2$CH$_2$PPh$_2$)$_2$] (**2a**)	−0.21 (s)	1.61 (dt)	13.2	5.4	−17.44 (dt)[a] [Ru–H]
	0.07 (s)	2.38 (dt)		3.9	
RuH(Cl)PPh$_3$[NH(SiMe$_2$CH$_2$PPh$_2$)$_2$] (**2b**)	−0.30 (s)	1.73 (dt)	13.1	5.0	−17.94 (dt)[b] [Ru–H]
	0.00 (s)	2.15 (dt)		4.7	
Ru(C$_6$H$_4$PPh$_2$)[N(SiMe$_2$CH$_2$PPh$_2$)$_2$] (**3**)	−0.19 (s)	1.90[c]	13.2	4.7	
	0.50 (s)			5.3	
RuCl(C$_6$H$_4$PPh$_2$)[NH(SiMe$_2$CH$_2$PPh$_2$)$_2$] (**4**)	−0.03 (s)	2.04 (dt)	13.6	5.1	3.74 (br s)
	0.01 (s)	2.32 (dt)		4.9	
RuH(PPh$_3$)[N(SiMe$_2$CH$_2$PPh$_2$)$_2$] (**5**)	−0.05 (s)	1.66[c]	13.1	3.8	−20.60 (dt)[d] [Ru–H]
	0.48 (s)			4.9	

[a] ^2J(H,P$_a$) = 21.2 Hz, ^2J(H,P$_b$) = 27.8 Hz. [b] ^2J(H,P$_a$) = 23.1 Hz, ^2J(H,P$_b$) = 25.2 Hz. [c] An AB quartet of virtual triplets. [d] ^2J(H,P$_a$) = 19.6 Hz, ^2J(H,P$_b$) = 41.5 Hz.

Table II. ^{31}P NMR Data

compd	P$_a$,[a] ppm	P_b,[a] ppm	^2J(P$_a$,P$_b$), Hz
RuCl(PPh$_3$)[N-(SiMe$_2$CH$_2$PPh$_2$)$_2$] (1)	5.65 (d)	50.5 (t)	32.8
RuH(Cl)PPh$_3$[NH-(SiMe$_2$CH$_2$PPh$_2$)$_2$] (**2a**)	33.3 (d)	68.2 (t)	35.7
RuH(Cl)PPh$_3$[NH-(SiMe$_2$CH$_2$PPh$_2$)$_2$] (**2b**)	31.9 (d)	55.9 (t)	35.5
Ru(C$_6$H$_4$PPh$_2$)[N-(SiMe$_2$CH$_2$PPh$_2$)$_2$] (**3**)	42.9 (d)	−5.9 (t)	27.9
RuCl(C$_6$H$_4$PPh$_2$)[NH-(SiMe$_2$CH$_2$PPh$_2$)$_2$] (**4**)	18.2 (d)	−7.0 (t)	32.8
RuH(PPh$_3$)[N(SiMe$_2$CH$_2$PPh$_2$)$_2$] (**5**)	48.6 (d)	93.8 (t)	31.3

[a] P$_a$ refers to the phosphorus nuclei in the tridentate ligand; P$_b$ refers to the phosphorus nucleus in the triphenylphosphine ligand.

Table III. Crystallographic Data[a]

compd	4·0.65PPh$_3$·0.35OPPh$_3$
formula	C$_{48}$H$_{51}$ClNP$_3$RuSi$_2$·C$_{18}$H$_{15}$O$_{0.35}$P
fw	1195.4
cryst syst	monoclinic
space group	$P2_1/n$
a, Å	9.8385 (5)
b, Å	29.561 (1)
c, Å	20.8665 (9)
β, deg	101.583 (4)
V, Å^3	5942.2 (5)
Z	4
ρ_c, g/cm^3	1.336
F(000)	2483.2
μ(Mo Kα), cm^{-1}	4.89
cryst dimens, mm	0.26 × 0.30 × 0.52
transmissn factors	0.781–0.886
scan type	ω–θ
scan range (in ω), deg	0.75 + 0.35 tan θ
scan speed, deg/min	1.8–20.0
data collected	$+h,+k,\pm l$
$2\theta_{max}$, deg	55
cryst decay	negligible
no. of unique rflns	13 566
no. of rflns with $I \geq 3\sigma(I)$	7906
no. of variables	689
R	0.030
R_w	0.037
S	1.154
mean Δ/σ (final cycle)	0.002
max Δ/σ (final cycle)	0.073
residual density, e/Å^3	−0.31 to +0.38

[a] Temperature 294 K, Enraf-Nonius CAD4-F diffractometer, Mo Kα radiation ($\lambda_{K\alpha_1}$ = 0.709 30, $\lambda_{K\alpha_2}$ = 0.713 59 Å), graphite monochromator, takeoff angle 2.7°, aperture (2.0 + tan θ) × 4.0 mm at a distance of 173 mm from the crystal, scan range extended by 25% on both sides for background measurement, $\sigma^2(I) = C + 2B + [0.04(C - B)]^2$ (C = scan count, B = normalized background count), function minimized $\Sigma w(|F_o| - |F_c|)^2$ where $w = 1/\sigma^2(F)$, $R = \sum||F_o| - |F_c||/\sum|F_o|$, $R_w = (\sum w(|F_o| - |F_c|)^2/\sum w|F_o|^2)^{1/2}$, $S = (\sum w(|F_o| - |F_c|)^2/(m - n))^{1/2}$. Values given for R, R_w, and S are based on those reflections with $I \geq 3\sigma(I)$.

NMR spectra were recorded on a Varian XL-300 (121.42 MHz) instrument and were referenced to external P(OMe$_3$)$_3$ set at +141.0 ppm relative to 85% H$_3$PO$_4$.

RuCl(PPh$_3$)[N(SiMe$_2$CH$_2$PPh$_2$)$_2$] (1). RuCl$_2$(PPh$_3$)$_3$ (0.60 g, 0.63 mmol) was dissolved in THF (60 mL), and a solution of LiN(SiMe$_2$CH$_2$PPh$_2$)$_2$ (0.34 g, 0.63 mmol) in THF (10 mL) was added. The mixture was stirred under N$_2$ for 24 h before the THF was removed in vacuo. The residue was extracted with hexane (~100 mL total) and filtered through Celite to remove LiCl. The solvent was removed in vacuo, leaving a red-brown solid, which was recrystallized from hexane–toluene at -20 °C; yield 0.36 g (62%). Anal. Calcd for C$_{48}$H$_{51}$ClNP$_3$RuSi$_2$: C, 62.16; H, 5.54; N, 1.51. Found: C, 62.04; H, 5.75; N, 1.53.

RuCl(PPh$_3$)H[NH(SiMe$_2$CH$_2$PPh$_2$)$_2$] (2). RuCl(PPh$_3$)[N-(SiMe$_2$CH$_2$PPh$_2$)$_2$] (1; 70 mg, 0.075 mmol) was dissolved in toluene (5 mL), and the resulting solution was stirred under a pressure of 1 atm of H$_2$ for 6 h. The solution turned light orange. The solvent was pumped off, and addition of hexane to the residue caused a yellow solid to precipitate. The solid was collected by filtration and washed with hexane and diethyl ether; yield 62 mg (89%). Anal. Calcd for C$_{48}$H$_{53}$ClNP$_3$RuSi$_2$: C, 62.02; H, 5.75; N, 1.51. Found: C, 62.23; H, 5.90; N, 1.60.

Ru(C$_6$H$_4$PPh$_2$)[N(SiMe$_2$CH$_2$PPh$_2$)$_2$] (3). RuCl(PPh$_3$)[N-(SiMe$_2$CH$_2$PPh$_2$)$_2$] (1; 110 mg, 0.12 mmol) was dissolved in THF (3 mL). The solution was cooled to 0 °C, and a solution of allylmagnesium bromide in THF (0.8 M, 0.15 mL, 0.12 mmol) was added dropwise. The solution was stirred for $^3/_4$ h at 0 °C and then warmed to room temperature. The solvent was pumped off and the residue extracted with hexane (~20 mL) and filtered through Celite. Hexane was removed from the filtrate by rotary evaporation, yielding a red solid. The solid was recrystallized from hexane–toluene; yield 97 mg (92%). Anal. Calcd for C$_{48}$H$_{50}$NP$_3$RuSi$_2$: C, 64.70; H, 5.66; N, 1.57. Found: C, 64.77; H, 5.66; N, 1.31.

RuCl(C$_6$H$_4$PPh$_2$)[NH(SiMe$_2$CH$_2$PPh$_2$)$_2$] (4). RuCl-(PPh$_3$)[N(SiMe$_2$CH$_2$PPh$_2$)$_2$] (1; 0.120 g, 0.13 mmol) was taken up in hexane (~15 mL). Triethylphosphine (20 mg, 0.17 mmol) was added dropwise, and the red-brown solution was stirred for 12 h. The product appeared as a yellow solid precipitating from a green solution. The product was collected by filtration and washed with cold hexane; yield 50 mg (42%). Anal. Calcd for C$_{66}$H$_{66}$ClNP$_4$RuSi$_2$O: C, 65.74; H, 5.52; N, 1.16. Found: C, 65.50; H, 5.45; N, 1.22.

RuH(PPh$_3$)[N(SiMe$_2$CH$_2$PPh$_2$)$_2$] (5). Ru(C$_6$H$_4$)PPh$_2$[N-(SiMe$_2$CH$_2$PPh$_2$)$_2$] (3; 100 mg, 0.11 mmol) was taken up in toluene (10 mL). The solution was stirred under 1 atm of H$_2$ for 24 h. The solvent was pumped off, and the residue was extracted with hexane. Cooling the hexane solution to -20 °C yielded a red solid, yield 85 mg (85%). Anal. Calcd for C$_{48}$H$_{52}$NP$_3$RuSi$_2$: C, 64.55; H, 5.87; N, 1.57. Found: C, 62.94; H, 5.78; N, 1.32.

X-ray Crystallographic Analysis of RuCl(C$_6$H$_4$PPh$_2$)-[NH(SiMe$_2$CH$_2$PPh$_2$)$_2$] (4). Crystallographic data are presented in Table III. The final unit cell parameters were obtained by least squares on 2(sin θ)/λ values for 25 reflections (2θ = 35–43°) measured with Mo Kα_1 radiation. The data were corrected for Lp and absorption (analytical method).[7]

Table IV. Final Positional (Fractional, ×10^4; Ru, ×10^6; Cl, P, Si, ×10^5) and Isotropic Thermal Parameters ($U \times 10^3$ Å^2) with Estimated Standard Deviations in Parentheses

atom	x	y	z	U_{eq}/U_{iso}
Ru	315949 (22)	320874 (7)	427152 (10)	29
Cl	21133 (9)	28477 (3)	51859 (4)	49
P(1)	31585 (8)	24592 (3)	38427 (3)	36
P(2)	35469 (7)	39248 (2)	48198 (3)	32
P(3)	14980 (7)	34733 (3)	34521 (3)	33
P(4)	66798 (13)	1650 (4)	36506 (6)	74
Si(1)	58798 (9)	24752 (3)	48199 (4)	45
Si(2)	61942 (8)	34366 (3)	54456 (4)	40
N	5194 (3)	2991 (1)	5033 (1)	37
C(1)	4280 (3)	2143 (1)	4504 (1)	43
C(2)	5433 (3)	3967 (1)	5029 (1)	37
C(3)	3932 (3)	2323 (1)	3129 (1)	41
C(4)	3918 (3)	2631 (1)	2632 (1)	45
C(5)	4485 (3)	2523 (1)	2089 (1)	52
C(6)	5063 (3)	2109 (1)	2038 (2)	54
C(7)	5095 (4)	1802 (1)	2525 (2)	64
C(8)	4526 (4)	1902 (1)	3068 (2)	61
C(9)	1598 (3)	2099 (1)	3665 (1)	39
C(10)	1075 (4)	1931 (1)	3045 (2)	57
C(11)	−57 (4)	1641 (1)	2932 (2)	67
C(12)	−678 (4)	1514 (1)	3435 (2)	64
C(13)	−186 (4)	1683 (1)	4056 (2)	62
C(14)	939 (3)	1974 (1)	4169 (2)	51
C(15)	3027 (3)	4468 (1)	4408 (1)	38
C(16)	3605 (3)	4603 (1)	3879 (1)	47
C(17)	3143 (4)	4998 (1)	3535 (2)	56
C(18)	2140 (4)	5258 (1)	3722 (2)	63
C(19)	1592 (4)	5136 (1)	4249 (2)	56
C(20)	2019 (3)	4742 (1)	4587 (1)	46
C(21)	3051 (3)	4031 (1)	5613 (1)	35
C(22)	3847 (3)	4303 (1)	6084 (2)	50
C(23)	3464 (4)	4384 (1)	6680 (2)	57
C(24)	2265 (4)	4205 (1)	6804 (2)	54
C(25)	1439 (4)	3949 (1)	6338 (2)	52
C(26)	1823 (3)	3855 (1)	5746 (1)	42
C(27)	6973 (4)	2548 (1)	4197 (2)	63
C(28)	6956 (4)	2197 (1)	5550 (2)	68
C(29)	8043 (3)	3396 (1)	5372 (2)	62
C(30)	6106 (4)	3408 (1)	6325 (2)	62
C(31)	2879 (3)	3680 (1)	3076 (1)	37
C(32)	3991 (3)	3511 (1)	3551 (1)	35
C(33)	5330 (3)	3596 (1)	3437 (1)	46
C(34)	5508 (4)	3830 (1)	2883 (2)	59
C(35)	4392 (4)	3989 (1)	2431 (2)	61
C(36)	3047 (3)	3913 (1)	2519 (1)	50
C(37)	316 (3)	3126 (1)	2855 (1)	36
C(38)	470 (3)	3061 (1)	2219 (1)	44
C(39)	−480 (4)	2799 (1)	1795 (1)	53
C(40)	−1593 (4)	2609 (1)	1992 (2)	60
C(41)	−1758 (4)	2672 (1)	2626 (2)	65
C(42)	−808 (3)	2926 (1)	3057 (2)	53
C(43)	297 (3)	3924 (1)	3564 (1)	36
C(44)	−17 (4)	4287 (1)	3137 (1)	49
C(45)	−971 (4)	4610 (1)	3238 (2)	62
C(46)	−1634 (4)	4571 (1)	3758 (2)	64
C(47)	−1336 (3)	4216 (1)	4180 (2)	54
C(48)	−368 (3)	3890 (1)	4088 (2)	45
C(49)	6938 (4)	−418 (1)	3928 (2)	61
C(50)	7230 (5)	−734 (1)	3485 (2)	71
C(51)	7425 (5)	−1184 (1)	3660 (2)	77
C(52)	7360 (5)	−1323 (1)	4274 (2)	75
C(53)	7100 (4)	−1013 (1)	4726 (2)	74
C(54)	6882 (4)	−561 (1)	4554 (2)	70
C(55)	7251 (4)	490 (1)	4398 (2)	66
C(56)	8662 (5)	504 (2)	4664 (3)	86
C(57)	9156 (5)	749 (2)	5228 (3)	96
C(58)	8292 (6)	987 (2)	5525 (2)	92
C(59)	6884 (6)	977 (2)	5270 (2)	88
C(60)	6376 (5)	728 (1)	4711 (2)	75
C(61)	4807 (5)	245 (1)	3492 (2)	68
C(62)	4275 (6)	626 (1)	3150 (2)	89
C(63)	2903 (7)	742 (2)	3054 (3)	102
C(64)	1998 (6)	464 (2)	3282 (3)	97
C(65)	2477 (6)	73 (2)	3605 (3)	102
C(66)	3874 (5)	−35 (2)	3706 (2)	86
O[a]	7336 (10)	294 (3)	3188 (4)	87
H(N)	4717 (29)	2929 (10)	5249 (13)	29 (9)

[a] Occupancy factor 0.35.

The structure was solved by Patterson and Fourier methods. In addition to the complex **4**, the asymmetric unit of the structure was found to contain a partially oxidized PPh_3 molecule. The occupancy factor of the O atom was initially refined with the thermal parameter fixed at 1.2 times that of P(4). In the final stages of refinement the occupancy factor of the oxygen atom was set at the value determined as described above and an anisotropic thermal parameter was refined. The amine hydrogen, H(N), was refined with an isotropic thermal parameter, and all other hydrogens were fixed in idealized positions (staggered methyls, C(sp^2)–H = 0.97 Å; C(sp^3)–H = 0.98 Å, $U_H \propto U_{\text{bonded atom}}$). Neutral atom scattering factors and anomalous dispersion corrections (Ru, Cl, P, Si) were taken from ref 8.

Final positional and equivalent isotropic thermal parameters ($U_{eq} = {}^1/_3 \operatorname{tr} U_{diag}$) are given in Table IV. Selected bond lengths and angles appear in Tables V and VI, respectively. Complete tables of bond lengths and angles, calculated hydrogen atom parameters, anisotropic thermal parameters, torsion angles, and structure factors (Tables V(S), VI(S), and VII–XI) and a plot of the (O)PPh_3 molecule are included as supplementary material.

Table V. Selected Bond Lengths (Å) with Estimated Standard Deviations in Parentheses

Ru–Cl	2.5736 (7)	P(4)–C(49)	1.819 (4)
Ru–P(1)	2.3892 (8)	P(4)–C(55)	1.821 (4)
Ru–P(2)	2.3998 (7)	P(4)–C(61)	1.821 (5)
Ru–P(3)	2.2545 (7)	P(4)–O	1.320 (7)
Ru–N	2.380 (2)	Si(1)–N	1.760 (3)
Ru–C(32)	2.054 (3)	Si(1)–C(1)	1.859 (3)
P(1)–C(1)	1.839 (3)	Si(1)–C(27)	1.858 (4)
P(1)–C(3)	1.848 (3)	Si(1)–C(28)	1.863 (4)
P(1)–C(9)	1.844 (3)	Si(2)–N	1.762 (3)
P(2)–C(2)	1.823 (3)	Si(2)–C(2)	1.875 (3)
P(2)–C(15)	1.843 (3)	Si(2)–C(29)	1.860 (3)
P(2)–C(21)	1.844 (3)	Si(2)–C(30)	1.855 (3)
P(3)–C(31)	1.806 (3)	N–H(N)	0.74 (3)
P(3)–C(37)	1.837 (3)	C(31)–C(32)	1.412 (4)
P(3)–C(43)	1.827 (3)	C(32)–C(33)	1.407 (4)

Results and Discussion

Synthesis of Ruthenium(II) Amides. The reaction of $RuCl_2(PPh_3)_3$ with the lithium amide–bis(phosphine) $LiN(SiMe_2CH_2PPh_2)_2$ in THF proceeds smoothly to give the ruthenium(II) amide complex $RuCl(PPh_3)[N(SiMe_2CH_2PPh_2)_2]$ (**1**; eq 2). Ruthenium amides are not that common.[9] In fact, only three other reports of mo-

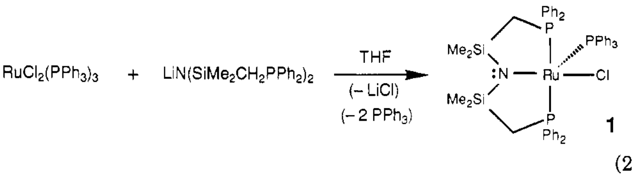

(2)

---

(7) The computer programs used include locally written programs for data processing and locally modified versions of the following: ORFLS, full-matrix least squares, and ORFFE, function and errors, by W. R. Busing, K. O. Martin, and H. A. Levy; FORDAP, Patterson and Fourier syntheses, by A. Zalkin; ORTEP II, illustrations, by C. K. Johnson; AGNOST, absorption corrections, by J. A. Ibers.

(8) *International Tables for X-ray Crystallography*; Kynoch Press: Birmingham, U.K., 1974; Vol. IV, pp 99–102, 149 (present distributor D. Reidel, Dordrecht, The Netherlands).

(9) Fryzuk, M. D.; Montgomery, C. D. *Coord. Chem. Rev.* **1989**, *95*, 1.

Table VI. Selected Bond Angles (deg) with Estimated Standard Deviations in Parentheses

Cl-Ru-P(1)	85.56 (3)	C(31)-P(3)-C(43)	111.7 (1)
Cl-Ru-P(2)	93.53 (2)	C(37)-P(3)-C(43)	99.0 (1)
Cl-Ru-P(3)	111.63 (3)	C(49)-P(4)-C(55)	103.2 (2)
Cl-Ru-N	78.55 (7)	C(49)-P(4)-C(61)	104.6 (2)
Cl-Ru-C(32)	178.69 (8)	C(49)-P(4)-O	116.7 (4)
P(1)-Ru-P(2)	169.88 (3)	C(55)-P(4)-C(61)	102.4 (2)
P(1)-Ru-P(3)	95.29 (3)	C(55)-P(4)-O	111.2 (4)
P(1)-Ru-N	86.34 (6)	C(61)-P(4)-O	117.1 (4)
P(1)-Ru-C(32)	95.74 (8)	N-Si(1)-C(1)	101.9 (1)
P(2)-Ru-P(3)	94.41 (3)	N-Si(1)-C(27)	112.4 (2)
P(2)-Ru-N	83.61 (6)	N-Si(1)-C(28)	111.1 (1)
P(2)-Ru-C(32)	85.19 (8)	C(1)-Si(1)-C(27)	112.4 (1)
P(3)-Ru-N	169.77 (7)	C(1)-Si(1)-C(28)	111.0 (2)
P(3)-Ru-C(32)	68.24 (8)	C(27)-Si(1)-C(28)	108.0 (2)
N-Ru-C(32)	101.56 (10)	N-Si(2)-C(2)	105.5 (1)
Ru-P(1)-C(1)	103.58 (10)	N-Si(2)-C(29)	111.8 (2)
Ru-P(1)-C(3)	122.31 (10)	N-Si(2)-C(30)	108.4 (2)
Ru-P(1)-C(9)	123.25 (10)	C(2)-Si(2)-C(29)	108.8 (1)
C(1)-P(1)-C(3)	102.2 (1)	C(2)-Si(2)-C(30)	113.8 (2)
C(1)-P(1)-C(9)	102.0 (1)	C(29)-Si(2)-C(30)	108.6 (2)
C(3)-P(1)-C(9)	100.0 (1)	Ru-N-Si(1)	112.3 (1)
Ru-P(2)-C(2)	103.34 (10)	Ru-N-Si(2)	115.9 (1)
Ru-P(2)-C(15)	122.90 (9)	Ru-N-H(N)	86 (2)
Ru-P(2)-C(21)	122.18 (9)	Si(1)-N-Si(2)	124.5 (1)
C(2)-P(2)-C(15)	103.1 (1)	Si(1)-N-H(N)	105 (2)
C(2)-P(2)-C(21)	102.4 (1)	Si(2)-N-H(N)	104 (2)
C(15)-P(2)-C(21)	99.9 (1)	P(1)-C(1)-Si(1)	109.6 (2)
Ru-P(3)-C(31)	87.28 (9)	P(2)-C(2)-Si(2)	110.3 (1)
Ru-P(3)-C(37)	125.72 (9)	Ru-C(32)-C(31)	107.5 (2)
Ru-P(3)-C(43)	123.07 (9)	Ru-C(32)-C(33)	136.5 (2)
C(31)-P(3)-C(37)	108.9 (1)		

nonuclear amides of Ru(II) have been published. The preparation of $RuH(PPh_3)_2[N(SiMe_3)_2]$[10] from $LiN(SiMe_3)_2$ and $Ru(H)Cl(PPh_3)_3$ and the synthesis of $Cp^*Ru(PMe_3)_2[NR(Ph)]$[11] (R = H, Ph) from LiNRPh and $Cp^*RuCl(PMe_3)_2$ describe well-characterized, authentic ruthenium amides. There is also a report[12] of the preparation of $Ru(NO)Cl_2(PPh_3)_2(NEt_2)$ from $RuCl_3 \cdot xH_2O$ and Et_2NNO in the presence of excess PPh_3; however, this assignment was based only on elemental analysis and the observation of a N-O stretching frequency in the IR spectrum.

The tridentate ligand system described here utilizes the soft nature of the phosphine groups present to stabilize the hard amido donor group toward the soft ruthenium(II) center. In addition, the lack of β-hydrogens on the amido ligand eliminates the possibility of β-elimination, a common reactivity for metal amides.[13]

Diagnostic of complex 1 is the $^{31}P\{^1H\}$ NMR spectrum, which shows a doublet and a triplet for the ancillary phosphine donors and the PPh_3 ligand, respectively (Table II). In the ^1H NMR spectrum of 1, one observes two singlets due to the silyl methyl groups ($Si(CH_3)_2$) and two doublets of virtual triplets corresponding to the methylene protons (PCH_2Si) of the backbone of the ligand (Table I). This inequivalence of the silyl methyl groups and the methylene protons along with the presence of virtual coupling is consistent with a meridional coordination mode (i.e., trans phosphine donors for the tridentate ligand).[14] However, no further stereochemical information may be gleaned from the NMR data, i.e., square-pyramidal (sqp) vs trigonal-bipyramidal (tbp) geometry. While both geometries are possible for five-coordinate d^6 complexes, theoretical[15] and solid-state structural studies[16] have shown square pyramidal to be generally the preferred geometry. Exceptions seem to occur when strong σ-donors are present, as they prefer[17] the equatorial sites of a *distorted* trigonal-bipyramidal geometry.[18] The presence of a chloride ligand, a good double-faced π-donor, as in 1 is known to favor the sqp geometry.[17] On the basis of the analogous structure of $RuCl_2(PPh_3)_3$, which has trans chlorides and a unique PPh_3 in the apical position of a slightly distorted sqp geometry, we propose that the structure of 1 is similar, having the PPh_3 ligand apical and the chloride trans to the amide nitrogen of the ligand backbone. Such a geometry is consistent with the rather large chemical shift difference of 1.18 ppm for the methylene proton signals (Table I); it is the largest such difference yet observed for this ligand system in a five-coordinate environment.[19] One might expect that the degree of inequivalence in environments on either side of the meridional plane of the tridentate ligand would be reflected in the peak positions of the methylene protons. Thus, a PPh_3 ligand in the apical position with its anisotropic phenyl substituents compared with an open sixth site would represent completely different chemical environments and be reflected in a large chemical shift difference in the methylene protons. While chemical shift arguments must always be approached with caution, there is corroborating evidence for this particular stereochemistry from reactivity studies (vide infra).

Activation of Dihydrogen. When $RuCl_2(PPh_3)_3$ is treated with H_2 in the presence of a base such as NEt_3, $Ru(H)Cl(PPh_3)_3$ is obtained along with $Et_3NH^+Cl^-$.[1] By analogy, when 1 was treated with dihydrogen, the coordinated amide acted as a base, giving the amine-hydride complex 2, $RuCl(PPh_3)H[NH(SiMe_2CH_2PPh_2)_2]$. The ^1H and ^{31}P NMR spectra reveal that two isomers, **2a** and **2b**, are actually present in a 2:1 ratio (**2a**:**2b**), as shown in eq 3. The N-H resonances in the ^1H NMR spectrum were observed as broad singlets at 4.25 and 3.84 ppm for **2a** and **2b**, respectively. In both of these isomers, the tridentate ligand retains the meridional stereochemistry, on the basis of the ^1H NMR spectral parameters, since doublets of virtual triplets are observed for the resonances of methylene protons; this requirement leaves just three possible arrangements of the remaining three ligands (disregarding

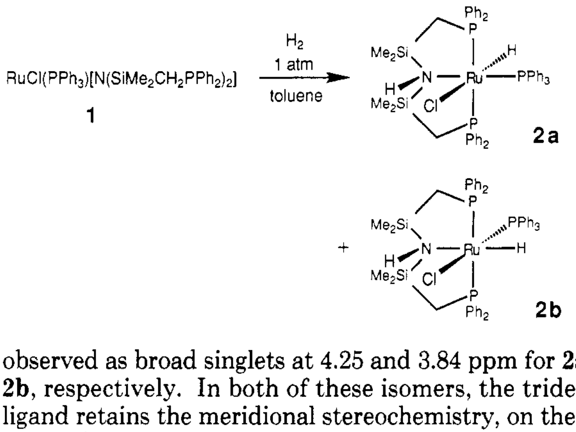

(3)

---

[10] Cetinkaya, B.; Lappert, M. F.; Torroni, S. *J. Chem. Soc., Chem. Commun.* **1979**, 843.

[11] Brynzda, H. E.; Fong, L. K.; Paciello, R. C.; Tam, W.; Bercaw, J. E. *J. Am. Chem. Soc.* **1987**, *109*, 1444.

[12] Khan, M. I.; Agarwala, U. C. *Bull. Chem. Soc. Jpn.* **1986**, *59*, 1285.

[13] Diamond, S. E.; Mares, F. *J. Organomet. Chem.* **1977**, *142*, C55.

[14] Brookes, P. R.; Shaw, B. L. *J. Chem. Soc. A* **1967**, 1079.

[15] (a) Pearson, R. G. *J. Am. Chem. Soc.* **1969**, *91*, 4947. (b) Rossi, A. R.; Hoffman, R. *Inorg. Chem.* **1975**, *14*, 365. (c) Burdett, J. K. *Inorg. Chem.* **1975**, *14*, 375. (d) *Ibid.* **1975**, *14*, 931. (e) Elian, M.; Hoffman, R. *Inorg. Chem.* **1975**, *14*, 1058.

[16] Holmes, R. R. *Prog. Inorg. Chem.* **1984**, *32*, 119.

[17] Thorn, D. L.; Hoffmann, R. *Nouv. J. Chim.* **1979**, *3*, 39.

[18] Fryzuk, M. D.; MacNeil, P. A.; Ball, R. G. *J. Am. Chem. Soc.* **1986**, *108*, 6414.

[19] (a) Fryzuk, M. D.; MacNeil, P. A.; Massey, R. L.; Ball, R. G. *J. Organomet. Chem.* **1989**, *368*, 231. (b) Fryzuk, M. D.; Joshi, K. *Organometallics* **1989**, *8*, 722.

the stereochemistry imposed by the amine N–H ligand). The geometry having the hydride ligand trans to triphenylphosphine can be excluded on the basis of the fact that neither isomer of **2** displays a large phosphorus to hydride coupling constant ($^2J_{PH}$) typical for a trans PPh_3 to hydride relationship; couplings are in fact typical of a cis relationship between these two ligands (Table I). This leaves the two geometric isomers shown in eq 3. However, the assignment of which geometry corresponds to the major and minor isomers respectively is more difficult. The major isomer has been tentatively assigned as having the stereochemistry with the PPh_3 ligand trans to the amine and the amine N–H and chloride ligand syn to each other, as illustrated by **2a** in eq 3. This assignment is supported by an alternate preparation of **2a**, which will be discussed later.

Consideration of the two observed isomers does not provide any information about which mechanism, concerted heterolytic cleavage of dihydrogen or oxidative addition followed by reductive elimination, might be operative. Indeed, the presence of the minor isomer **2b**, having the hydride and amine groups mutually trans, is difficult to explain with use of either mechanism. In fact, the stereoisomer that would be most easily explained by both mechanisms would be the unobserved third possible isomer, having the hydride and the triphenylphosphine donors mutually trans (this assumes that the stereochemical arrangement of **1** is in fact square pyramidal with the triphenylphosphine in the apical position).

One explanation that rationalizes these results is that the overall reaction of the ruthenium amide complex **1** with dihydrogen is not kinetically controlled; rather, the isomer ratio is a consequence of a sequence proceeding under thermodynamic control. This is consistent with both the known relative trans influences of the triphenylphosphine, hydride, chloride, and amine ligands (trans influence decreases in the order $PPh_3 > H > Cl \approx$ amine)[20] and perhaps the presence of an intramolecular hydrogen bond between the amine N–H and the chloride ligand. This latter interaction was initially observed by us for some iridium and rhodium complexes containing this ligand system upon reaction with H_2.[4] That **2a** is favored over **2b** may reflect the less severe steric interactions when the triphenylphosphine is trans to the amine as in **2a** as compared to cis as in **2b**.

Ortho Metalation and Related Reactions. Since the presence of the chloride ligand leads to complications (i.e., formation of an intramolecular hydrogen bond), we attempted to prepare the analogous hydrocarbyl complexes by metathesis of the chloride **1** with LiR (R = Me, CH_2SiMe_3). However, the compound isolated was the product of ortho metalation of the triphenylphosphine ligand, $Ru(C_6H_4PPh_2)[N(SiMe_2CH_2PPh_2)_2]$ (**3**; eq 4). Likewise, when the Grignard reaction C_3H_5MgBr was used, **3** was obtained.

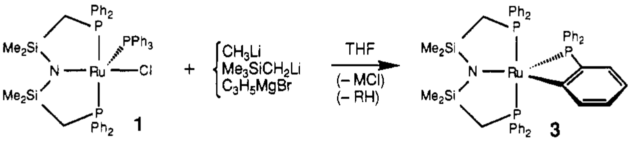

(4)

The suspicion that orthometalation of PPh_3 had occurred was readily confirmed by the $^{31}P\{^1H\}$ NMR spectrum of **3**. In the case of complexes **1** and **2a**,**b**, chemical shift of the triphenylphosphine ligand falls in the range of +50.5 to +68.2 ppm (Table II). By comparison in **3**, the signal appears at −5.0 ppm. This upfield shift upon ortho metalation has been observed previously.[21] The propensity for the PPh_3 ligand to ortho metalate is well-known for not only complexes of Ru(II)[22] but other metals as well.[23]

Once again meridional coordination of the tridentate ancillary ligand is evident by the presence of virtual coupling in the methylene proton signals. The only other stereochemical information available from the NMR data comes from the inequivalence of the silyl methyl groups and the methylene on either side of the tridentate ligand. However, in this case the replacement of a π-donor group (chloride) of **1** with a strong σ-donor (phenyl group) in **3** would be expected to favor a trigonal-bipyramidal geometry, as previously mentioned. Consistent with this prediction, the chemical shift difference between the doublets of virtual triplets observed for the resonances of the methylene protons, which was so large in the case of **1**, has decreased to the point that an overlapping AB quartet of virtual triplets is now observed (Table I).

To avoid this ortho metalation side reaction, we attempted to substitute the PPh_3 ligand of **1** with PEt_3. Addition of a slight excess of PEt_3 to **1** resulted in the formation of the new complex **4**, having the same molecular formula as **1** but with a $^{31}P\{^1H\}$ NMR spectrum that indicated ortho metalation had occurred (Table II). As shown in eq 5, **4** has the formula $RuCl(C_6H_4PPh_2)[NH(SiMe_2CH_2PPh_2)_2]$. The amine hydrogen (N–H) is again observed as a broad singlet at 3.74 ppm in the ^1H NMR spectrum. Suitable crystals of **4** were obtained for a single-crystal X-ray diffraction study, the details of which are described in a following section. The structure of **4** in solution is entirely consistent with the solid-state structure and is that shown in eq 5 with the tridentate ligand meridional and the ortho-metalated carbon trans to the chloride.

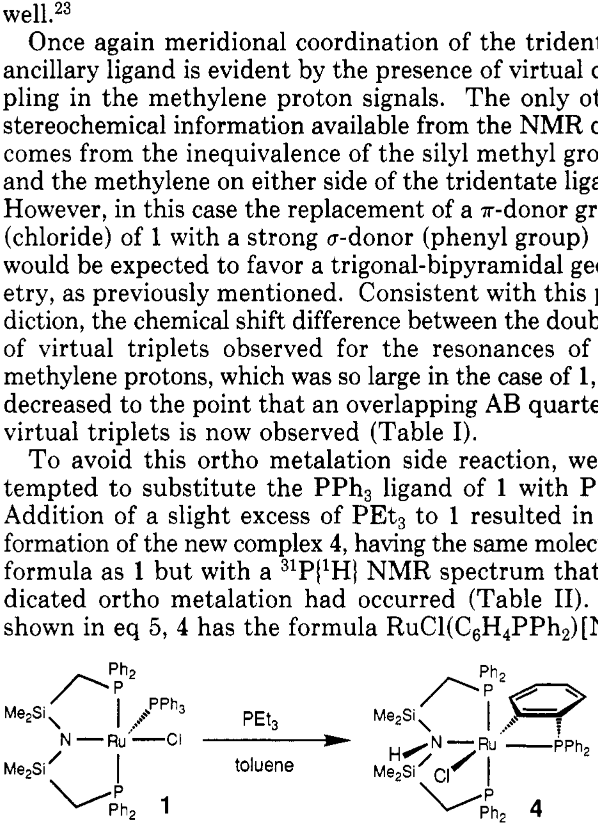

(5)

It is possible to relate the structure of **4** to the initially proposed structure of the starting complex **1** by the following mechanism: coordination of PEt_3 to the open site of the square-pyramidal geometry of **1** would force the trans PPh_3 ligand in closer proximity[24] to the amide nitrogen, thus assisting removal of the ortho hydrogen atom. Dissociation of the PEt_3 and rearrangement lead to the observed product. This rearrangement deserves some comment. One can speculate that the amine donor dissociates, undergoes inversion, and recoordinates concomitant with the chloride moving to a cis disposition to the amine. It should be noted that we also see the production

---

[20] Appleton, T. G.; Clark, H. C.; Manzer, L. E. *Coord. Chem. Rev.* **1973**, *10*, 335.

[21] Cole-Hamilton, D. J.; Wilkinson, G. *J. Chem. Soc., Dalton Trans.* **1977**, 797.

[22] (a) Cole-Hamilton, D. J.; Wilkinson, G. *Nouv. J. Chim.* **1977**, *1*, 141. (b) James, B. R.; Markham, L. D.; Wang, D. K. W. *J. Chem. Soc., Chem. Commun.* **1974**, 439.

[23] (a) McKinney, R. J.; Knobler, C. B.; Huie, B. T.; Kaesz, H. D. *J. Am. Chem. Soc.* **1977**, *99*, 2988. (b) Perego, G.; Del Piero, G.; Cesari, M.; Clerici, M. G.; Perrotti, E. *J. Organomet. Chem.* **1973**, *54*, C51.

[24] Structurally characterized square-pyramidal geometries normally have the metal above the plane defined by the four basal ligands, thus causing the apical ligand to be further from any of its cis neighbors as compared to a pure octahedral environment.

of this ortho-metalated product 4 upon crystallization of the starting complex 1 over extended periods. In this case, the excess PPh_3 liberated in the reaction of the lithium amide $LiN(SiMe_2CH_2PPh_2)_2$ with $RuCl_2(PPh_3)_3$ presumably weakly coordinates and induces the same transformation, but more slowly.

Both of the ortho-metalated complexes 3 and 4 were found to react with H_2. Complex 4 on exposure to 1 atm of H_2 is converted to a complex whose ^1H NMR spectrum is identical with that tentatively assigned earlier to complex **2a**. None of the other isomer **2b** (eq 3) was detectable.

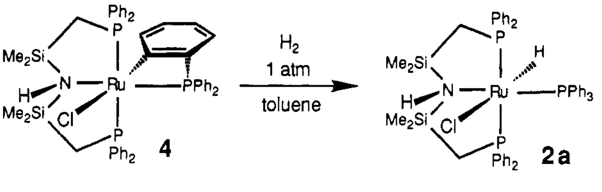

(6)

This reaction provides some support for the proposed stereochemistry assigned to **2a**, as the triphenylphosphine ligand remains trans to the amino group upon reaction.

When the ortho-metalated complex 3 is exposed to 1 atm of H_2, it is converted to the monohydride amide 5 (eq 7).

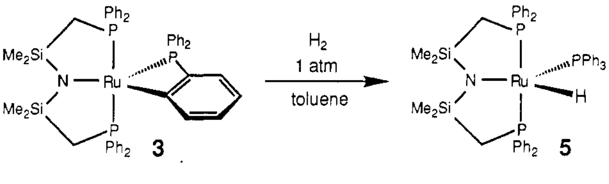

(7)

The hybrid tridentate ligand is again coordinated in a meridional fashion. We assume a simple trigonal-bipyramidal geometry because of the presence of strong σ-donors (i.e., hydride and PPh_3) in the equatorial position and the observed small chemical shift difference between the methylene protons, resulting in an overlapping AB quartet of virtual triplets. Interestingly, no further reaction is observed with excess H_2; this is in contrast to the iridium(III) dihydride complex $IrH_2[N(SiMe_2CH_2PPh_2)_2]$, which adds 1 equiv of H_2 to generate the thermally labile trihydride–amine derivative *mer*-$IrH_3[NH(SiMe_2CH_2PPh_2)_2]$.[25]

X-ray Crystal Structure Description. The geometry of the complex 4 was found to be octahedral, with the tridentate ligand bound in a skewed, meridional fashion and the chloride ligand trans to the ortho-metalated phenyl of the triphenylphosphine, as shown in Figure 1.

The Ru–P bond distances (2.3892 (8) and 2.3998 (7) Å) for the tridentate ligand of 4 are considerably different from that to P(3) in the coordinated triphenylphosphine (2.2545 (7) Å). Presumably this is due to the high trans influence of phosphines relative to that of amines. These distances are comparable to those in $RuCl_2(PPh_3)_3$.[26] In that structure, the two mutually trans triphenylphosphine ligands exhibit Ru–P distances of 2.374 (6) and 2.388 (7) Å, while the third phosphine trans to the open site in the pseudooctahedron has an Ru–P distance of 2.230 (8) Å. The Ru–Cl distance in 4 of 2.5736 (7) Å is likewise lengthened by the high trans influence of the ortho-metalated aryl group. This is confirmed by comparison to the structure of $[Ru(PPh_3)_2(CO)(CSe)Cl_2]$, where the two chlorides, positioned trans to the high-trans-influence CO and CSe ligands, have Ru–Cl distances of 2.478 (6) and 2.477 (7) Å, respectively.[27]

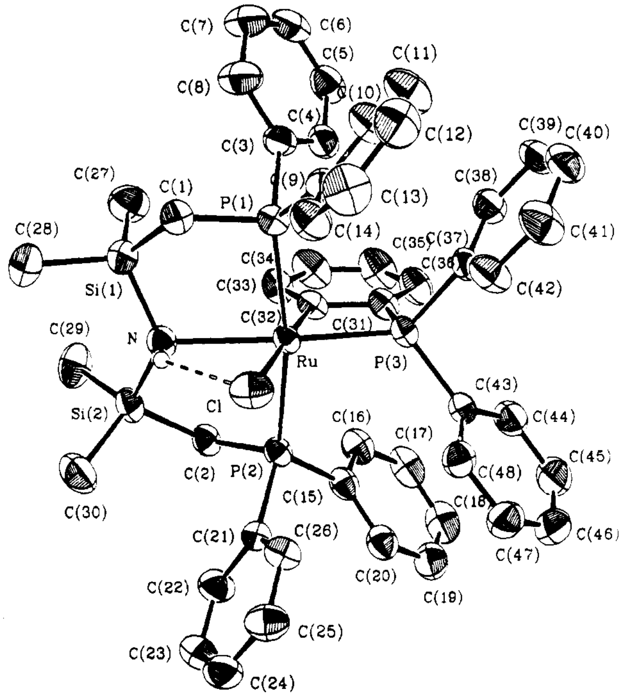

Figure 1. Molecular structure and atom-labeling scheme for $RuCl(C_6H_4PPh_2)[NH(SiMe_2CH_2PPh_2)_2]$ (4).

While cyclometalation is a common phenomenon, there is only one other example of a structurally characterized, ortho-metalated triphenylphosphine on ruthenium(II), and that is in $K[RuH_2(C_6H_4PPh_2)(PPh_3)_2]$.[28] In this ruthenate complex, the Ru–C distance is 2.098 (11) Å and is slightly longer than the observed distance of 2.054 (3) Å in 4, presumably reflecting trans-influence differences between PPh_3 and Cl in the respective complexes. The angles in the four-membered ring of the metallacycle are typical of other such rings in the literature; for example, the above-mentioned ruthenate has C–Ru–P = 67.6 (3)°, while in 4 this angle is 68.24 (8)°.

Perhaps the most interesting feature of the structure is the presence of a hydrogen bond between the amine and chloride ligands. The N–H distance is 0.74 (3) Å, while the NH···Cl distance is 2.55 (3) Å. These distances are shorter than those found in other complexes of rhodium and iridium that also incorporate this ligand system and display this intramolecular hydrogen bonding,[4] suggesting that this intramolecular hydrogen bond is especially strong. The N–H distances in such complexes range from 0.70 (8) to 0.83 (4) Å, while the NH···Cl distance was previously reported to be 2.76 (6) Å.[4] Certainly, the NH···Cl distance in 4 is considerably shorter than the expected van der Waals separation of 3.0 Å.[29] Such a contraction of the NH···X distance has been found in previous studies of hydrogen-bonded complexes.[30] Perhaps the best indication of the presence of a bonding interaction between the hydrogen and chlorine is the fact that the amine hydrogen lies in the plane of N, Cl, and Ru, thus minimizing the NH···Cl distance. By a similar reasoning one would also expect the N–H···Cl angle to be near-linear; however, in this system the contraints of the tridentate ligand, of which

---

(25) Fryzuk, M. D.; MacNeil, P. A. *Organometallics* **1983**, *2*, 682.

(26) (a) La Placa, S. J.; Ibers, J. A. *Inorg. Chem.* **1965**, *4*, 778. (b) Hoffman, P. R.; Caulton, K. G. *J. Am. Chem. Soc.* **1975**, *97*, 4221.

(27) Clark, G. R.; James, S. M. *J. Organomet. Chem.* **1977**, *134*, 229.

(28) Pez, G. P.; Grey, R. A.; Corsi, J. *J. Am. Chem. Soc.* **1981**, *103*, 7528.

(29) Bondi, A. *J. Phys. Chem.* **1964**, *68*, 441.

(30) Bronty, C.; Spinat, P.; Whuler, A. *Acta Crystallogr., Sect. B* **1980**, *36*, 1967.

the amine group is a part, disallow this. Thus, the observed N–H–Cl angle is only 138 (3)°.

Conclusions

A number of new five-coordinate ruthenium amide complexes have been prepared, all incorporating the tridentate $^{-}N(SiMe_2CH_2PPh_2)_2$. The complex $RuCl(PPh_3)[N(SiMe_2CH_2PPh_2)_2]$ (**1**) displays some unique reactivity patterns. Especially noteworthy is the conversion of the amide linkage of **1** to an amine via two distinct pathways: addition of H_2 to produce the isomeric amine chlorides $RuCl(PPh_3)H[NH(SiMe_2CH_2PPh_2)_2]$ (**2a**,**b**) and activation of an ortho C–H bond of the PPh_3 unit to generate $RuCl(C_6H_4PPh_2)[NH(SiMe_2CH_2PPh_2)_2]$ (**4**). The driving force for both of these reactions appears to be the formation of an intramolecular hydrogen bond between the amine N–H and the coordinated chloride. Attempts to introduce hydrocarbyl groups via metathesis of the chloride ligand of **1** with use of ortholithium or Grignard reagents were unsuccessful, resulting in the facile ortho metalation of the PPh_3 group to generate $Ru(C_6H_4PPh_2)[N(SiMe_2CH_2PPh_2)_2]$ (**3**).

Acknowledgment. We thank the NSERC of Canada for financial support in the form of operating grants to M.D.F. and a Postdoctoral Fellowship to C.D.M. Johnson Matthey is gratefully acknowledged for a generous loan of $RuCl_3$. We also thank Professor Brian James for helpful discussions.

Supplementary Material Available: Complete tables of bond lengths and angles, calculated hydrogen atom parameters, anisotropic thermal parameters, and torsion angles (Tables V(S), VI(S), and VII–X) and a plot of the $(O)PPh_3$ molecule (14 pages); a table of structure factors (Table XI) (59 pages). Ordering information is given on any current masthead page.

Photochemically Reactive Polymers: Synthesis and Characterization of Polyurethanes Containing $Cp_2Mo_2(CO)_6$ or $Cp_2Fe_2(CO)_4$ Molecules along the Polymer Backbone

Steve C. Tenhaeff and David R. Tyler*

Department of Chemistry, University of Oregon, Eugene, Oregon 97403

Received June 25, 1990

The syntheses of oligomeric urethanes containing Mo–Mo or Fe–Fe bonds along the backbone are reported. Reaction of the organometallic "diol" $(\eta^5\text{-}C_5H_4C(O)CH_2OH)_2Mo_2(CO)_6$ with $OCN(CH_2)_6NCO$ (hexamethylene diisocyanate; HMDI) gave $[-OCH_2C(O)C_5H_4(CO)_3Mo-Mo(CO)_3C_5H_4C(O)CH_2OC(O)NH(CH_2)_6NHC(O)-]_n$ (n = 4–5). Similarly, reaction of $(\eta^5\text{-}C_5H_4CH_2CH_2OH)_2Mo_2(CO)_6$ with HMDI gave $[-OCH_2CH_2C_5H_4(CO)_3Mo-Mo(CO)_3C_5H_4CH_2CH_2OC(O)NH(CH_2)_6NHC(O)-]_n$ (n = 6–8) and reaction of $(\eta^5\text{-}C_5H_4CH_2CH_2OH)_2Fe_2(CO)_4$ with HMDI gave $[-OCH_2CH_2C_5H_4(CO)_2Fe-Fe(CO)_2C_5H_4CH_2CH_2OC(O)NH(CH_2)_6NHC(O)-]_n$ (n = 2–3). A copolymer with a lower density of metal–metal bonds along the backbone was synthesized by reacting $(\eta^5\text{-}C_5H_4CH_2CH_2OH)_2Mo_2(CO)_6$ and $HO(CH_2)_4OH$ with HMDI. The polyurethanes were characterized by elemental analysis, by infrared, ^1H NMR, and electronic absorption spectroscopy, and by molecular weight. With certain preparations, $\bar{M}_n$ values up to 16 000 ($n \simeq 20$) were obtained. As an aid to the spectroscopic characterization of the complexes, model complexes were synthesized by reacting *mono*isocyanates with the metal–metal bonded diols. For example, $[CH_3(CH_2)_5NHC(O)OCH_2CH_2C_5H_4(CO)_3Mo-Mo(CO)_3C_5H_4CH_2CH_2OC(O)NH(CH_2)_5CH_3]$ was synthesized by reacting $(\eta^5\text{-}C_5H_4CH_2CH_2OH)_2Mo_2(CO)_6$ with $CH_3(CH_2)_5NCO$. Because of the metal–metal bonds along the backbone, the polyurethanes are photochemically reactive, undergoing metal–metal bond photolysis reactions similar to the $Cp_2Mo_2(CO)_6$ and $Cp_2Fe_2(CO)_4$ dimers.

Introduction

Reactive polymers are a major new area of polymer synthesis and technology. Such polymers can be used in a variety of technological applications. For example, recent reports describe the use of reactive polymers as catalysts,[1–9] ion-exchange resins,[10] selective chelating agents,[6,11–13] polymeric supports,[2–6,8,9] and permselective materials.[10] One subset of the reactive polymer area is the field of

---

(1) Grubbs, R. H.; Shiu-Chiu, H. S. In *Organometallic Polymers*; Carraher, C. E., Jr., Sheats, J. E., Pittman, C. U., Jr., Eds.; Academic Press: New York, 1978; pp 129–134.

(2) Karol, F. J. In *Organometallic Polymers*; Carraher, C. E., Jr., Sheats, J. E., Pittman, C. U., Jr., Eds.; Academic Press: New York, 1978; pp 135–143.

(3) Lang, W. H.; Jurewicz, A. T.; Haag, W. O.; Whitehurst, D. D.; Rollmann, L. D. In *Organometallic Polymes*; Carraher, C. E., Jr., Sheats, J. E., Pittman, C. U., Jr., Eds.; Academic Press: New York, 1978; pp 145–154.

(4) Gray, H. B. In *Organometallic Polymers*; Carraher, C. E., Jr., Sheats, J. E., Pittman, C. U., Jr., Eds.; Academic Press: New York, 1978; pp 155–164.

(5) Zeldin, M.; Fife, W. K.; Cheng-xiang, T.; Jian-Min, X. In *Inorganic and Organometallic Polymers*; Zeldin, M., Wynne, K. J., Allcock, H. R., Eds.; ACS Symposium Series 360; American Chemical Society: Washington, DC, 1988; Chapter 15.

(6) Neckers, D. C. In *Metal-Containing Polymeric Systems*; Sheats, J. E., Carraher, C. E., Jr., Pittman, C. U., Jr., Eds.; Plenum Press: New York, 1985; pp 385–403.

(7) Bailar, J. C., Jr. In *Organometallic Polymers*; Carraher, C. E., Jr., Sheats, J. E., Pittman, C. U., Jr., Eds.; Academic Press: New York, 1978; pp 313–321.

(8) Bergbreiter, D. E. *CHEMTECH* 1987, 686.

(9) Macomber, D. W.; Hart, W. P.; Rausch, M. D. In *Advances in Organometallic Chemistry*; Stone, F. G. A., West, R., Eds.; Academic Press: New York, 1982; pp 1–55.

(10) *Chemical Reactions on Polymers*; Benham, J. L., Kinstle, J. F., Eds.; ACS Symposium Series 364; American Chemical Society: Washington, DC, 1988.

(11) Okamoto, Y.; Wang, S. S.; Zhu, K. J.; Banks, E.; Garetz, B.; Murphy, E. K. In *Metal-Containing Polymeric Systems*; Sheats, J. E., Carraher, C. E., Jr., Pittman, C. U., Jr., Eds.; Plenum Press: New York, 1985; pp 425–450.

(12) Archer, R. D.; Hardiman, C. J.; Kim, K. S.; Grandbois, E. R.; Goldstein, M. In *Metal-Containing Polymeric Systems*; Sheats, J. E., Carraher, C. E., Jr., Pittman, C. U., Jr., Eds.; Plenum Press: New York, 1985; pp 355–366.

(13) Archer, R. D.; Wang, B.; Tramontano, V. J.; Lee, A. Y.; Orchaya, V. O. In *Inorganic and Organometallic Polymers*; Zeldin, M., Wynne, K. J., Allcock, H. R., Eds.; ACS Symposium Series 360; American Chemical Society: Washington, DC, 1988; Chapter 37.

0276-7333/91/2310-0473$02.50/0